

# Free expansion of Bose-Einstein condensates with quantized vortices

Franco Dalfovo<sup>1</sup> and Michele Modugno<sup>2</sup>

<sup>1</sup>*Dipartimento di Fisica, Università di Trento, and Istituto Nazionale per la Fisica della Materia, Unità di Trento, I-38050 Povo, Italy*

<sup>2</sup>*Dipartimento di Fisica, Università di Firenze, and Istituto Nazionale per la Fisica della Materia, Unità di Firenze,*

*Largo E. Fermi 2, I-50125 Firenze, Italy*

(Received 7 July 1999; published 14 January 2000)

The expansion of Bose-Einstein condensates with quantized vortices is studied by solving numerically the time-dependent Gross-Pitaevskii equation at zero temperature. For a condensate initially trapped in a spherical harmonic potential, we confirm previous results obtained by means of variational methods showing that, after releasing the trap, the vortex core expands faster than the radius of the atomic cloud. This could make the detection of vortices feasible, by observing the depletion of the density along the axis of rotation. We find that this effect is significantly enhanced in the case of anisotropic disk-shaped traps. The results obtained as a function of the anisotropy of the initial configuration are compared with the analytic solution for a noninteracting gas in three dimensions as well as with the scaling law predicted for an interacting gas in two dimensions.

PACS number(s): 03.75.Fi, 05.30.Jp

## INTRODUCTION

Since the discovery of Bose-Einstein condensation in trapped gases of alkali-metal atoms [1], one of the primary goals of both experimental and theoretical activity has been the search for superfluid effects. A clean connection among Bose-Einstein condensation and superfluidity would be, in fact, of fundamental importance from a conceptual viewpoint, for it would improve our understanding of the properties of quantum many-body systems. In this context, attempts have been made to produce and detect quantized vortices in these trapped gases [2] and experiments are currently running in different laboratories. At the same time, several theoretical papers have been written on the expected features of these vortices (see, for instance, Refs. [3–6] and references therein).

One of the difficulties in observing a vortex in a trapped condensate is that its core, i.e., the region where the density is depleted by the centrifugal force associated with the quantized vorticity, has a radius of the order of the healing length  $\xi$ . This quantity is significantly smaller than the radius of the cloud, especially when the number of atoms,  $N$ , is large. This makes a direct observation rather difficult, due to the finite resolution of the optical imaging devices.

Among the various methods suggested for detecting vortices, one consists in letting the condensate expand freely by switching off the trapping potential. It has recently been shown [7] that the core of the vortex may expand faster than the radius of the cloud, making the observation of the corresponding density depletion feasible. In order to give quantitative estimates of this effect, in Ref. [7] the Gross-Pitaevskii equation has been solved by using an approximate trial wave function and the vortex core size has been studied in the case of a gas initially confined in a spherical trap.

In the present work we study the same problem, namely the dynamics of the expanding condensate with a vortex inside, by exactly solving the Gross-Pitaevskii equation and exploring also the effects of the anisotropy of the initial configurations. Our calculations for the spherical case closely agree with the results of Ref. [7], showing that the magnifi-

cation of the core size is not an artifact of the variational wave function used by those authors. In the case of anisotropic configurations, we find different behaviors depending on the form of the trap. When the initial confinement is weaker along the axis of rotation (cigar-shaped traps) the axial expansion is slower, while the radial one is similar to that of a two-dimensional (2D) condensate: the core size and the radius of the cloud increase with almost the same speed, following the scaling behavior expected for the solutions of the Gross-Pitaevskii equation in 2D [8]. Conversely, when the initial confinement is stronger along the axis of rotation (disk-shaped traps), the axial expansion is faster and the core size is found to increase much more than the radius of the cloud in the first instants of motion. The ratio between the radii of the core and the cloud starts from a rather small value, which depends on  $N$  and is close to the prediction for a 2D condensate, and then increases quickly to the value 0.282, which is the analytic result for an ideal gas in 3D. All these results will be discussed in detail in Sec. III, while in the next section we will introduce the basic formalism and the numerical procedure.

## SOLVING THE GROSS-PITAEVSKII EQUATION

The dynamics of a dilute and weakly interacting Bose-Einstein condensate at zero temperature is well described by a mean-field theory, in which the motion of all the atoms is assumed to be determined by a single complex function  $\Phi(\mathbf{r}, t)$ , also called the order parameter, playing the role of a macroscopic wave function and obeying the following equation:

$$i\hbar \frac{\partial}{\partial t} \Phi(\mathbf{r}, t) = \left[ -\frac{\hbar^2 \nabla^2}{2m} + V_{\text{ext}}(\mathbf{r}) + g|\Phi(\mathbf{r}, t)|^2 \right] \Phi(\mathbf{r}, t). \quad (1)$$

This is known as the Gross-Pitaevskii (GP) equation [9]. The mean-field interaction enters through the term proportional to the particle density  $n(\mathbf{r}, t) = |\Phi(\mathbf{r}, t)|^2$ , the coupling constant  $g$  being related to the  $s$ -wave scattering length  $a$  by  $g = 4\pi\hbar^2 a/m$ . For an axially symmetric trap the confining

potential  $V_{\text{ext}}(\mathbf{r})$  can be written in the form  $V_{\text{ext}}(\rho, z) = (m/2)[\omega_\rho^2 \rho^2 + \omega_z^2 z^2]$ , with  $\rho = (x^2 + y^2)^{1/2}$ . The ratio between the axial ( $\omega_z$ ) and radial ( $\omega_\rho$ ) frequencies,  $\lambda = \omega_z/\omega_\rho$ , is a useful parameter fixing the anisotropy of the trap. The derivation and several applications of the GP equation (1) are reviewed in Ref. [5].

In general, the order parameter entering the GP equation (1) can be written in the form

$$\Phi(\mathbf{r}, t) = \sqrt{n(\mathbf{r}, t)} \exp[iS(\mathbf{r}, t)] \quad (2)$$

where the phase  $S(\mathbf{r}, t)$  can be used to define a velocity field through

$$\mathbf{v}(\mathbf{r}, t) = (\hbar/m) \nabla S(\mathbf{r}, t). \quad (3)$$

When a quantized vortex is present in the condensate, with its axis of rotation along  $z$ , the atoms flow with tangential velocity  $v = \kappa \hbar / (m\rho)$ , each one having angular momentum  $L_z = \kappa \hbar$ , where  $\kappa$  is the quantum of circulation. This means that, from Eq. (3), the order parameter has to depend on the angle  $\phi$ , around the  $z$  axis, in a simple way:

$$\Phi(\mathbf{r}, t) = \Psi(\rho, z, t) \exp[i\kappa\phi]. \quad (4)$$

Inserting this expression back into the GP equation (1), one gets

$$i\hbar \frac{\partial}{\partial t} \Psi(\rho, z, t) = [-\hbar^2 \nabla^2 / 2m + \kappa^2 \hbar^2 / 2m\rho^2 + (m/2)(\omega_\rho^2 \rho^2 + \omega_z^2 z^2) + g|\Psi(\rho, z, t)|^2] \Psi(\rho, z, t), \quad (5)$$

which corresponds to the GP equation with a centrifugal force included. Due to this centrifugal term, the solution  $\Psi(\rho, z, t)$  must vanish on the  $z$  axis. The region where the density is depleted, close to the the vortex line, is named vortex core. In a stationary state, its radius is of the order of the healing length  $\xi$  fixed by the balance between the mean-field energy and the kinetic energy associated with the gradient of the density (quantum pressure). In a uniform gas, the healing length is given by  $\xi = (8\pi na)^{-1/2}$ , where  $n$  is the density. One can use the same expression in order to estimate the core size in trapped gases by taking for  $n$  the central density of the condensate without vortices. With the parameters of the current experiments, the predicted core radius turns out to be very small indeed, making the direct observation of a vortex rather difficult with the presently available optical devices. However, when the condensate is allowed to expand by switching off the confining potential, the vortex core expands as well. We want to describe this process by numerically solving Eq. (5).

The GP equation (5) can be formally rewritten in the following way:

$$i\hbar (\partial \Psi / \partial t) = H \Psi, \quad (6)$$

where the effective Hamiltonian  $H$  is the operator enclosed in square brackets in Eq. (5). Equation (6) has the form of a nonlinear Schrödinger equation, since  $H$  contains the unknown  $\Psi$ . There exist several techniques to solve it numeri-

cally. One of them consists in propagating the wave function in time using small time steps  $\Delta t$  in order to approximate the time evolution of  $\Psi$  with the equation

$$[1 + (i\Delta t/2)H] \Psi_{n+1} = [1 - (i\Delta t/2)H] \Psi_n, \quad (7)$$

where  $H$  and  $\Psi_n$  are the effective Hamiltonian and the order parameter, respectively, both calculated at the  $n$  iteration. Actually, since the diffusion of  $\Psi$  occurs in both the axial and radial directions, one splits each time interval in two parts, one for the evolution along  $z$  and the other along  $\rho$ . In order to propagate  $\Psi$  in each direction, we separate the effective Hamiltonian into axial and radial components, equally dividing the mean-field potential (this separation is somewhat arbitrary and does not affect the final results). Equation (7), for both the axial and radial motion at each time step, can be solved by mapping the order parameter on a two-dimensional grid of points,  $N_\rho \times N_z$ , in such a way that its solution becomes equivalent to a matrix diagonalization. This is known as the Crank-Nicholson differencing method with an alternating direction implicit algorithm [10] and was used for the expansion of a trapped condensate first by Holland and Cooper [11].

For a vortex in a trap with radial frequency  $\omega_\rho$ , the relevant length scale is  $a_\rho = [\hbar / (m\omega_\rho)]^{1/2}$ . Available condensates have radii of the order of  $(1-10) a_\rho$ , depending on the strength of the mean-field interaction fixed by the parameter  $Na/a_\rho$  [5]. We consider condensates with repulsive interaction ( $a > 0$ ) and with  $Na/a_\rho$  from 0 to 20. We choose a grid having typically  $100 \times 200$  points with spacing smaller than  $0.2a_\rho$ , which is sufficient for an accurate description of the density profile of the condensate including the vortex core. The derivatives in the effective Hamiltonian  $H$  are expressed through finite-difference five-point formulas [12].

The initial configuration at  $t=0$  corresponds to the stationary order parameter of the condensate in the trap for a given  $\kappa$ . It can be obtained by using the same algorithm, but diffusing the function  $\Psi$  in imaginary time instead of real time ( $t \rightarrow -i\tau$ ). One starts from a reasonable trial wave function and lets  $\Psi$  converge to the stationary state. The same can be done by using an explicit differencing algorithm instead of the implicit one based on Eq. (7). The explicit method has been used, for instance, in Ref. [13] and turns out to be much faster. We used both methods as a test of the numerical code.

For  $t > 0$ , the confining potential in Eq. (5) is removed and hence the function  $\Psi$  expands freely, subject only to the mean-field repulsion and quantum pressure. A CPU time of the order of 2 h on a workstation is typically needed to follow the expansion of the condensate for a time of the order of  $10\omega_\rho^{-1}$ , which is enough to see the effects that we are going to discuss.

The expansion of an ideal gas ( $a=0$ ) is used as one of the tests we made on the numerics. In this case, one has simple analytic results. The  $t=0$  configurations are the eigenstates of the harmonic oscillator in axial symmetry. The  $\kappa=0$  case is a Gaussian, while the vortex state  $\kappa=1$  corresponds to the eigenfunction with azimuthal angular momentum  $m=1$ . When the trap is released, their expansion is just the disper-

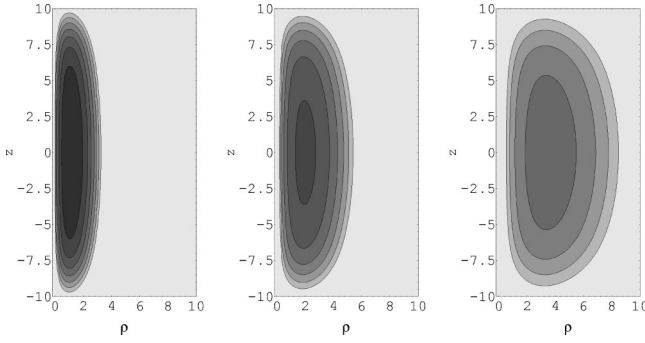


FIG. 1. Contour plot of the density  $n(\rho, z, t) = |\Psi(\rho, z, t)|^2$  in three instants of time [from left to right,  $t = (0, 1.5, 3)\omega_\rho^{-1}$ ] for a condensate with  $\lambda = \omega_z/\omega_\rho = 0.2$  and  $Na/a_\rho = 20$  and having a quantized vortex ( $\kappa = 1$ ) along the  $z$  axis. The darkest color represents the region where the density is larger than  $\frac{1}{2}$  of the peak density at  $t = 0$ , and each contour line is drawn where the density falls by a factor 2. The coordinates  $z$  and  $\rho$  are given in units of  $a_\rho = [\hbar/(m\omega_\rho)]^{1/2}$ , where  $\omega_\rho$  is the radial trapping frequency at  $t = 0$ .

sion of free wave packets. We checked that our numerical integration gives results practically indistinguishable from the analytic ones. In order to verify the proper inclusion of the mean-field interaction in the code, we made the calculation for the expansion of a condensate without vortices, using the same parameters of a previous work [14] and finding exactly the same results. As a further check, we looked at the behavior of the energy of the condensate as a function of time. It is well known that the Crank-Nicholson method may suffer from a possible amplification of random numerical noise, due to nonlinearity, leading to a spurious input of kinetic energy and limiting the stability of the algorithm to short time. However, we checked that this time is long enough to ensure the stability of the solutions in the time intervals considered here.

## RESULTS

First we give two examples of expanding vortices. In Figs. 1 and 2 we show a sequence of contour plots of the density  $n(\rho, z, t) = |\Psi(\rho, z, t)|^2$  in three instants of time [ $t = (0, 1.5, 3)\omega_\rho^{-1}$ ] and for two different condensates ( $\lambda = 0.2$  and  $2.5$ , respectively). The darkest color represents the region where the density is larger than  $1/2$  of the peak density at  $t = 0$ , and each contour line is drawn where the density

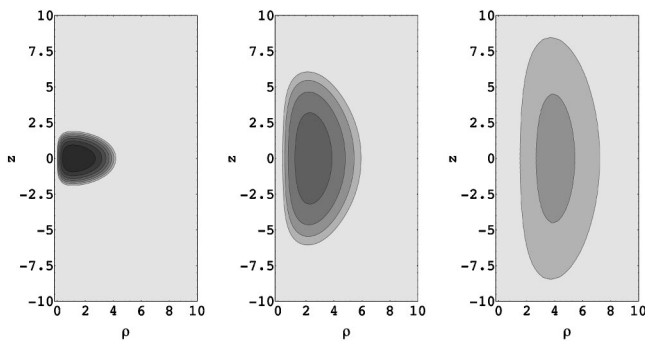


FIG. 2. Same as in Fig. 1 but for a condensate in a trap with  $\lambda = \omega_z/\omega_\rho = 2.5$ .

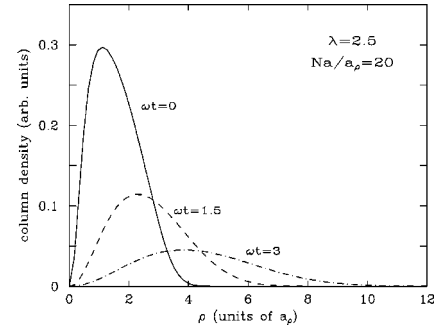


FIG. 3. Column density  $n(\rho, t)$  obtained by integrating along  $z$  the density plotted in Fig. 2. The three curves correspond to  $t = (0, 1.5, 3)\omega_\rho^{-1}$ .

falls by a factor 2. Both condensates have  $Na/a_\rho = 20$ , so that the effects of the mean-field interaction on the vortex structure are of the same order. The empty region close to  $\rho = 0$  is the vortex core, whose radius grows when the atomic cloud expands. The condensate in Fig. 1 is initially confined in a cigar-shaped trap. When the trap is released, its motion is mainly in the radial direction, the axial size increasing much more slowly [15]. The opposite happens for the condensate in Fig. 2: the initial configuration is oblate (disk-shaped) and the axial motion is faster.

The shape of the condensate is better seen by plotting the *column density*, that is, the density integrated along the  $z$  direction,  $n_{\text{col}}(\rho, t) = \int dz n(\rho, z, t)$ . This quantity is directly measured in the experiments. In Fig. 3, we plot  $n_{\text{col}}$  for the same expanding condensate shown in Fig. 2. To give an idea of the actual size, let us suppose we have a trap with frequency  $\omega_\rho = 2\pi$  (20 Hz) and condensates of  $^{87}\text{Rb}$  or Na atoms; then the length scale  $a_\rho$  is  $2.4 \mu\text{m}$  and  $4.7 \mu\text{m}$ , respectively. In the same cases, the parameters  $Na/a_\rho = 20$  and  $\lambda = 2.5$ , as in Fig. 3, would correspond to  $N \approx 8000$  for  $^{87}\text{Rb}$  and  $N \approx 34\,000$  for Na.

By using the column density, one can give suitable definitions of the radii of both the atomic cloud and the vortex core. The former can be identified with the root-mean-square radius,  $\rho_{\text{rms}}$ , obtained by integrating  $\rho^2$  over the column density distribution, while the core radius,  $\rho_c$ , can be chosen as the value of  $\rho$  where the column density first reaches  $e^{-1}$  times the peak value. It is then useful to study the evolution in time of the ratio  $\rho_c/\rho_{\text{rms}}$ , in order to have an estimate of the size of the ‘‘hole’’ made by a vortex in typical condensates of current experiments, as done in Ref. [7]. In Fig. 4 we show this ratio for different values of  $\lambda$  and  $Na/a_\rho$ . This figure contains the main results of the present work.

First, the horizontal dot-dashed line is the analytic result for the free dispersion of a wave packet of noninteracting particles. In this case, the motion in the two directions is decoupled and the ratio  $\rho_c/\rho_{\text{rms}}$  is approximately 0.282, independently of  $\lambda$ . The points close to this value correspond to the numerical solution of the GP equation (5) without the mean-field term ( $g = 0$ ). The fluctuations at short time are not due to random noise in the evolution of  $\Psi$ , which remains indeed very close to the analytic solution at any time, but to the smallness of the vortex core at the beginning of the expansion: both the position of the peak and that of  $\rho_c$  are located in between grid points, and the use of interpolation

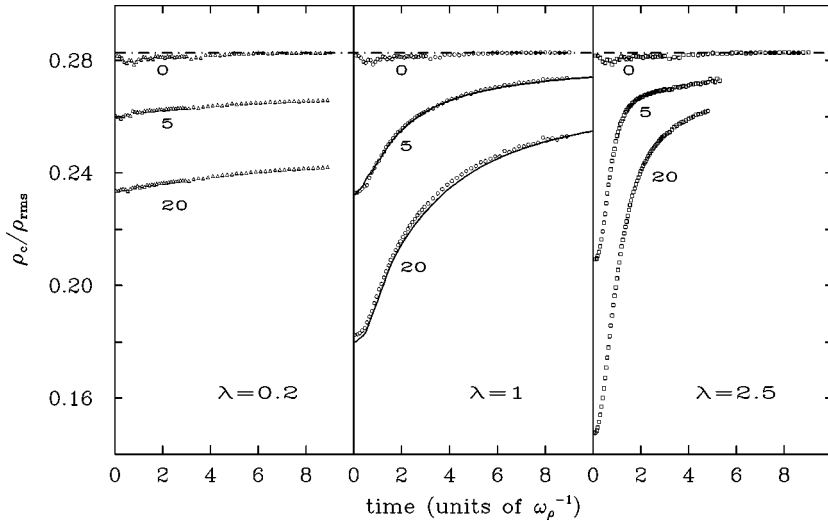


FIG. 4. Ratio between the vortex core radius and the root mean square radius of the condensate,  $\rho_c/\rho_{\text{rms}}$ , as a function of time, for three different initial configurations ( $\lambda=0.2, 1, 2.5$ ) and for  $Na/a_\rho=0, 5$ , and  $20$ . Time is in units of  $\omega_\rho^{-1}$ . Points are the numerical results of the present work. The horizontal dot-dashed line corresponds to the expansion of an ideal gas in the state  $m=1$ . The two solid lines for  $Na/a_\rho=5$  and  $20$  in the spherical case,  $\lambda=1$ , are the results of recent variational calculations [7].

formulas yields small errors. As one can see from the figure, these fluctuations are rather small and do not affect the main results of this work.

The results obtained by expanding condensates with  $Na/a_\rho=5$  and  $20$  are also shown. At  $t=0$ , each sequence of points starts from the value of  $\rho_c/\rho_{\text{rms}}$  predicted for a stationary state in the trap. This value is a decreasing function of both the parameters  $Na/a_\rho$  and  $\lambda$ . An estimate of this dependence can be obtained in the so-called Thomas-Fermi limit  $Na/a_\rho \gg 1$ , when quantum pressure is negligible compared to the mean-field repulsion. In this case, one finds  $\rho_c/\rho_{\text{rms}} \sim \xi/\rho_{\text{rms}} \propto (15\lambda Na/a_\rho)^{-2/5}$ . Thus the portion of the condensate where the density is depleted by the vortex becomes smaller and smaller when  $N$  and/or  $\lambda$  increase. This is why in current experiments the vortex core might be hardly observable by simply looking at the density distribution in the trap.

At  $t>0$ , the ratio  $\rho_c/\rho_{\text{rms}}$  increases in different ways depending on the anisotropy of the trap. In the case of a spherical trap ( $\lambda=1$ ), we compare the numerical solution of the GP equation (points) with the results of the variational calculation by Lundh, Pethick, and Smith [7] (solid lines). The

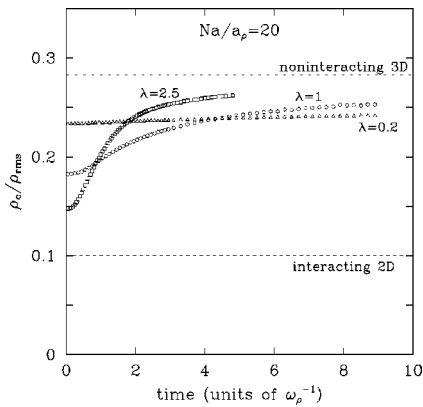


FIG. 5. Ratio  $\rho_c/\rho_{\text{rms}}$  as a function of time, for three different initial configurations ( $\lambda=0.2, 1, 2.5$ ) but the same value of  $Na/a_\rho=20$ . The dot-dashed line is the analytic result for an expanding ideal gas. The dashed line is the result obtained by solving the GP equation in a purely 2D system.

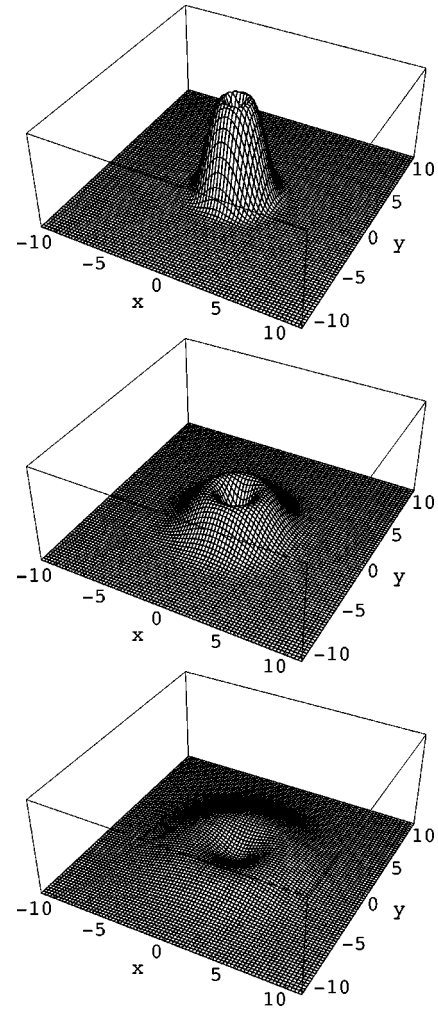


FIG. 6. The column density of Fig. 3 is shown here as a 3D plot in order to emphasize the structure of the expanding vortex. The three frames correspond again to  $t=(0, 1.5, 3)\omega_\rho^{-1}$ .



agreement is remarkable. The ratio  $\rho_c/\rho_{\text{rms}}$  is shown to increase rather quickly towards the analytic result for the non-interacting gas. As discussed in Ref. [7], this is due to the fact that, in the first instants of motion, the core size adjusts almost instantaneously to the value  $\xi = (8\pi na)^{-1/2}$ , with  $n$  given by the local density just outside the vortex core. This density decreases rapidly, yielding an increase of  $\rho_c$  faster than that of  $\rho_{\text{rms}}$ . After a characteristic decoupling time, this mean-field effect tends to vanish, since the gas becomes more and more dilute, and the condensate expands as an ideal gas, with the axial and radial motions decoupled. The ratio  $\rho_c/\rho_{\text{rms}}$  thus remains almost frozen to its value at the decoupling time.

As one can see in Fig. 4, the magnification of the core size depends on both  $Na/a_\rho$  and  $\lambda$ . In order to emphasize the dependence on the anisotropy of the trap, in Fig. 5 the results for  $Na/a_\rho = 20$  and different values of  $\lambda$  are plotted together. The lowest dashed line is the result we obtain by solving the GP equation in a purely 2D case with the same  $Na/a_\rho$ . In this case, one can prove that the dynamics is governed by an exact scaling law [8], that is, the condensate preserves its shape with a time dilatation of length scales; thus  $\rho_c/\rho_{\text{rms}}$  remains constant. Our results show that the ratio  $\rho_c/\rho_{\text{rms}}$  is almost constant even for condensates initially confined in prolate (cigar-shaped) traps, the value at  $t=0$  being fixed by the local density near the vortex in the stationary state. This can be understood by noticing that, for  $\lambda \ll 1$ , the axial motion is so slow that it does not affect significantly the behavior of the radial expansion. In other words, the lowering of the local density, which causes  $\rho_c$  to increase, is almost completely determined by the radial expansion; the condensate can be thought of as being made up of thin slices, orthogonal to the  $z$  axis, each one expanding as a 2D system. The opposite happens in the case of disk-shaped traps ( $\lambda \gg 1$ ),

where the initial value of  $\rho_c/\rho_{\text{rms}}$  is indeed close to that of a 2D system, but quickly approaches the 3D ideal gas prediction. This is again a consequence of the axial motion. In this case, in fact, the rapid decrease of the local density around the vortex is almost entirely due to the fast axial expansion and hence the core size increases much faster than in a 2D system.

The fact that the 2D scaling behavior applies to the expansion of cigar-shaped condensates rather than the disk-shaped ones was not obvious so far. For instance, in a recent paper by Castin and Dum [16] that focused on the properties of vortices in disk-shaped traps, the expansion of the condensate has been treated by keeping the confinement along  $z$  constant and using the 2D scaling law for the radial motion. However, as shown in the present work, the motion along  $z$  in the actual 3D experiments is not expected to be a small correction to the 2D scaling law. On the contrary, it is expected to dominate the dynamics of the expansion, yielding values of  $\rho_c/\rho_{\text{rms}}$  close to 0.282 in short time and almost independent of  $N$ . This may help the direct detection of quantized vortices in these inhomogeneous Bose-Einstein condensates, the size of the ‘‘hole’’ in the density distribution becoming easily larger than the spatial resolution of the imaging devices. In order to show how this expanding hole might appear in an experimental observation, the column density of Fig. 3 is plotted again in Fig. 6 as a 3D plot, the three frames corresponding to  $t = (0, 1.5, 3)\omega_\rho^{-1}$ .

#### ACKNOWLEDGMENTS

This work has been supported by Istituto Nazionale per la Fisica della Materia through the Advanced Research Project on BEC, and by Ministero dell’Università e della Ricerca Scientifica e Tecnologica. F.D. would like to thank the Aspen Center for Physics, where this work has been completed.

- 
- [1] M.H. Anderson *et al.*, Science **269**, 198 (1995); K.B. Davis *et al.*, Phys. Rev. Lett. **75**, 3969 (1995); C.C. Bradley *et al.*, *ibid.* **75**, 1687 (1995); **79**, 1170(E) (1997).
  - [2] W. Ketterle *et al.*, in *Proceedings of the International School of Physics ‘‘E. Fermi,’’* Course CXL, edited by M. Inguscio, S. Stringari, and C. Wieman (IOS Press, Amsterdam, 1999), p. 67.
  - [3] A.L. Fetter, in *Proceedings of the International School of Physics ‘‘E. Fermi’’* (Ref. [2]), p. 201.
  - [4] D.A. Butts and D.S. Rokhsar, Nature (London) **397**, 327 (1999).
  - [5] F. Dalfovo *et al.*, Rev. Mod. Phys. **71**, 463 (1999).
  - [6] S. Stringari, Phys. Rev. Lett. **82**, 4371 (1999).
  - [7] E. Lundh *et al.*, Phys. Rev. A **58**, 4816 (1998).
  - [8] Yu. Kagan *et al.*, Phys. Rev. A **54**, R1753 (1996); L. P. Pitaevskii and A. Rosch, *ibid.* **55**, R853 (1997).
  - [9] L.P. Pitaevskii, Zh. Eksp. Teor. Fiz. **40**, 646 (1961) [Sov. Phys. JETP **13**, 451 (1961)]; E.P. Gross, Nuovo Cimento **20**, 454 (1961).
  - [10] W.H. Press *et al.*, *Numerical Recipes* (Cambridge University Press, New York, 1986).
  - [11] M.J. Holland and J. Cooper, Phys. Rev. A **53**, R1954 (1996).
  - [12] *Handbook of Mathematical Functions*, edited M. Abramowitz and I. A. Stegun (Dover New York, 1972).
  - [13] F. Dalfovo and S. Stringari, Phys. Rev. A **53**, 2477 (1996).
  - [14] M.J. Holland *et al.*, Phys. Rev. Lett. **78**, 3801 (1997).
  - [15] Note that the apparent contraction of the condensate along  $z$  in Fig. 1 is an artifact of the contour plot. In fact, the density is decreasing during the expansion and thus the area within each contour line tends to decrease as well. The contour plot is suitable for representing the behavior of the aspect ratio (axial to radial size), but not for the absolute average size in each direction.
  - [16] Y. Castin and R. Dum, Eur. Phys. J. D **7**, 399 (1999).